

Relationship between Osteoinductive Characteristics of Biocomposite Material and Physicochemical Characteristics of Coating

M. Z. Fedorova, S. V. Nadezhdin, Yu. R. Kolobov,
M. B. Ivanov, N. A. Pavlov, and E. V. Zubareva

The osteoinductive characteristics of hydroxylapatite-based coating with different physicochemical characteristics were studied. The formation of the bone tissue on the studied types of the implant coating differed by the pattern and rate of formation of structural elements of the bone. Clear-cut phase-wise osteogenesis was seen on combined calcium phosphate coating: intense formation of the fibrous interstitial substance (due to cellular structure of hydroxylapatite) and slow maturing of cell elements. Bilayer composite coating provided (during the same period) the formation of more mature connective tissue. This phenomenon can be explained by better bioavailability of the coating material. The properties of combined calcium phosphate coating can be evaluated as mainly osteoconductive, while those of bilayer composite coating as osteoinductive.

Key Words: *hydroxyapatite; implant; osteoconduction; osteoinduction*

Implants from biocomposite material are more and more often used for repair of bone defects in orthopedics. This material consists of a metal base determining mechanical strength of the entire construction and bioactive coating with the structure, composition, and characteristics close to those of the bone tissue. One of these coating types is hydroxyapatite (HAP) [3,4,7,9,10]. It is assumed that in order to attain the optimal osteoinductive effects, the coating is to have a rough surface, branched network of canals and pores, and high strength with elasticity modulus close to that of the bone [1]. These physicochemical characteristics provide better growth of the bone tissue into the implant coating pores and channels [6,8].

We evaluated the osteoinductive characteristics of HAP-based coatings with different physicochemical characteristics.

MATERIALS AND METHODS

The implants were made from VT-6 titanium with two coating types based on HAP ($\text{Ca}_{10}(\text{PO}_4)_6(\text{OH})_2$) with crystals of nanostructure size in electrolyte and colloid solution: 10-20 nm wide and 100-150 nm long. Type 1 (combined calcium phosphate coating) was obtained by applying the nanostructural HAP from electrolyte solution (HAP concentration 0.5%) in parallel with microarc oxidation. This resulted in the formation of 8-10 μ thick coating with porous structure (1-3 μ pores). Type 2 coating (bilayer composite coating) was created by a series of steps. Colloid nanodispersed

HAP (HAP concentration 0.3%) was applied (by the sol gel method) onto porous TiO₂ layer formed by microarch oxidation. The 5-6 μ layer of nanocrystal HAP was smooth (slightly rough surface without porous structure), completely repeating the sublayer relief. The prepared samples were burned for 1 h: type 1 at 500°C, type 2 at 350°C.

Reparative osteogenesis at the site of HAP-coated titanium samples implantation was studied using direct inoculation of the implants into the tibial bone of laboratory albino rats. The study was carried out on 40 animals, divided at random into 3 groups: 2 experimental and 1 control groups. In animals narcotized with ether, the access to the tibial bone was made by a linear dissection. The muscle layer and the periosteum were dissected. A longitudinal hole was drilled on the anterior surface of the bone by a sterile bore. The sterile implant was placed into the resultant groove. The wound was sutured hermetically. A similar operation with adherence to all aseptic and antiseptic measures, but without implantation, was carried out in the control group. The animals were sacrificed on day 30 by ether overdosage. The bone was removed and the implantation zone was cut out. Bone fragments were fixed in 10% formalin. The implant in experimental animals was removed and dehydrated. The samples were examined in a Quanta 200 scanning electron microscope (SEM) in the low vacuum mode [2,5]. Fragments of the bones remaining after removal of the implants were decalcinated in 25% Trilon B solution and embedded in paraffin. The sections were stained with hematoxylin and eosin. Histological preparations were examined using a Video-Test-Size complex. The percentage of loose and coarse fibrous connective tissue, cartilage, reticulofibrous, and lamellar bone tissue was evaluated. The inflammatory and

immune reactions to implantation were evaluated by measuring plasma concentrations of C-reactive protein (CRP) and IL-1β in control and experimental rats on a Sunrize enzyme immunoassay analyzer (TECAN; measurements in the absorption mode at λ=450 nm). The following reagent kits for enzyme immunoassay were used: Rat C-Reactive Protein – ELISA Kit Cat. No. CYT294 (Chemicon) and IL-1β – Rat IL-1β – ELISA BMS630 (Bender MedSystems GmbH). The significance of differences was evaluated by Student's *t* test.

The study was carried out on the equipment of the Belgorod State University.

RESULTS

Scanning electron microscopy showed differences in the connective tissue structures forming on the surface of the implants with coating created by different methods. Chaotic fibrillar structures penetrating into the pores were detected on the implants with combined calcium phosphate coating; fine fibrillar formations and bone trabeculae were seen at sites of the implant surface contact with the bone (Fig. 1, *a*). The study of the implant—tissue contact areas in specimens with bilayer composite coating showed newly formed bone trabeculae without “free” fibrillar connective tissue structures (Fig. 1, *b*).

The findings of light microscopy confirmed the SEM findings. A thin layer of loose fibrillar connective tissue, more compact in the zone of the implant contact with combined calcium phosphate coating, was seen in histological preparations (Fig. 2). A layer of coarse fibrous connective tissue with fields of cartilage and new reticulofibrous bone tissue was seen around the capsular wall beyond a cord of loose connective

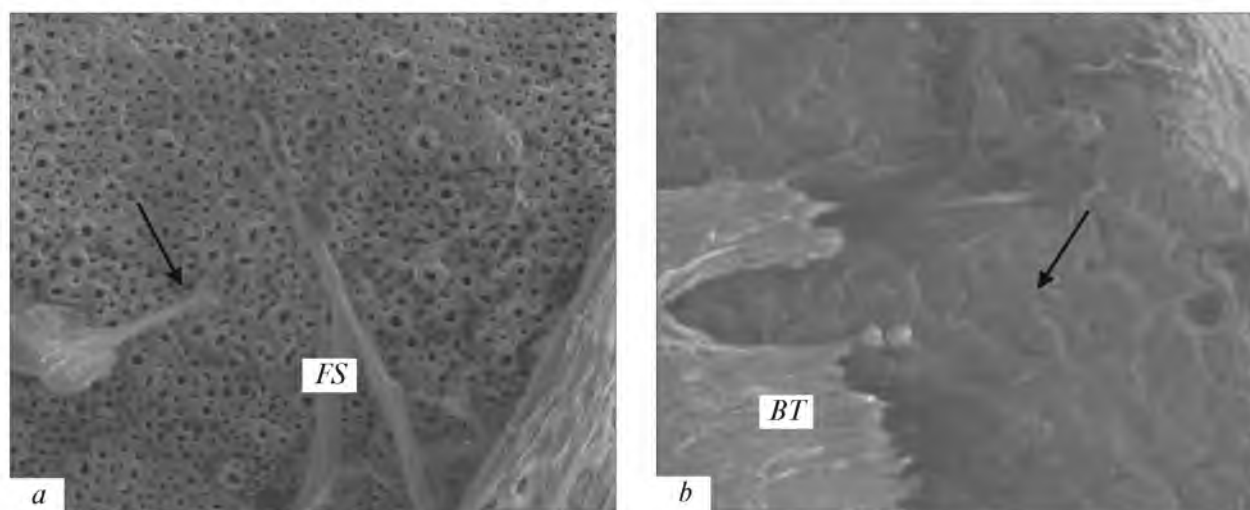


Fig. 1. Electronograms of implant surfaces. Arrow shows the coating surface. *a*) fibrillar structures (FS) on combined calcium phosphate coating, ×1500; *b*) bone trabeculae (BT) and surface of an implant with a bilayer composite coating, ×1000.

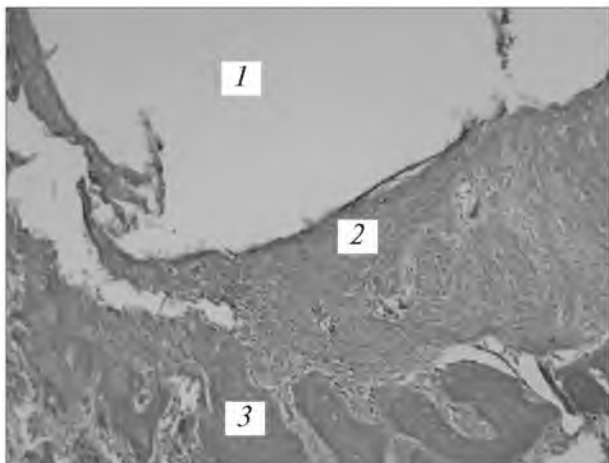


Fig. 2. Microphotograph of the site of implant inoculation. Implantation defect in the bone (1) surrounded by a layer of loose fibrous connective tissue (2). Reticulofibrous bone tissue (3). Hematoxylin and eosin staining, $\times 40$.

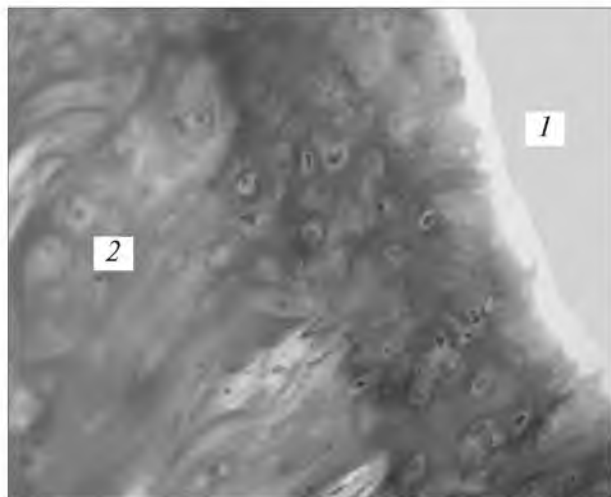


Fig. 3. Microphotograph of the site of implant inoculation. Implantation defect in the bone (1) with a fragment of new fine fibrillar bone tissue with osteocytes (2). Hematoxylin and eosin staining, $\times 400$.

tissue. The area of loose and coarse fibrous connective tissue was $5.0 \pm 0.2\%$, of cartilage $15.0 \pm 0.1\%$, of reticulofibrous bone tissue $60.0 \pm 0.4\%$, and of lamellar bone tissue $20.0 \pm 0.5\%$. New lamellar bone tissue with fine fibrillar structures predominated in histological preparations of implants with bilayer composite coating (Fig. 3). The volume of reticulofibrous bone tissue in these samples was $20.0 \pm 0.2\%$, of lamellar bone tis-

sue $80.0 \pm 0.4\%$; no loose or coarse fibrous connective tissue was detected.

Plasma concentrations of CRP and IL-1 β were virtually the same in control and experimental rats, which attested to the absence of inflammatory and immune reactions to the implant.

The study showed that bone tissue neof ormation on the studied types of the implant coating differed by the type and rate of formation of structural elements of the bone. Phase-wise osteogenesis was clearly seen on combined calcium phosphate coating: intense formation of fibrillar interstitium (due to cellular structure of HAP) and delayed maturing of cell elements. Bilayer coating provided the formation of more mature connective tissue during the same period. This phenomenon is due to better bioavailability of the coating material. The characteristics of combined calcium phosphate coating can be evaluated as mainly osteoconductive, while those of bilayer composite coating as osteoinductive ones.

The authors are grateful to D. A. Kolesnikov for scanning electron microscopy microphotographs made with the equipment of Center for Common Use at the Belgorod State University.

REFERENCES

1. V. I. Kalita, A. G. Gnedovets, A. I. Mamaev, *et al.*, *Fizika Khim. Obrabotki Mater.*, No. 3, 39-47 (2005).
2. G. I. Lavrishcheva and G. A. Onoprienko, *Morphological and Clinical Aspects of Reparative Regeneration of Supporting Organs and Tissues* [in Russian], Moscow (1996).
3. I. A. Khlusov, A. V. Kralov, N. S. Pozhen'ko, *et al.*, *Byull. Eksp. Biol. Med.*, **132**, No. 12, 107-112 (2001).
4. A. Shane, M. F. Catledge, K. Yogen, *et al.*, *Encyclopedia of Nanoscience and Nanotechnology*, Vol. 10, 1-22 (2003).
5. R. Müller, G. Gröger, K. A. Hiller, *et al.*, *Appl. Environ. Microbiol.*, **73**, No. 8, 2653-2660 (2007).
6. K. A. Hing, S. M. Best, K. E. Tanner, *et al.*, *J. Biomed. Mater. Res.*, **68**, No. 1, 187-200 (2004).
7. A. V. Karlov, Y. R. Kolobov, L. S. Busnev, *et al.*, *Med. Biol. Engin. Comp.*, **37**, No. 3, 198-199 (1999).
8. Y. R. Kolobov, A. V. Karlov, E. E. Sagymbaev, *et al.*, *Bioceramics*, **13**, 215-218 (2000).
9. S. H. Youn, Z. X. Yang, K. H. Hwang, and K. H. Grain, *Adv. Technol. Mater. Mater. Proc. J.*, **9**, 17-20 (2007).
10. N. A. Zakharov, I. A. Polunina, K. E. Polunin, *et al.*, *Inorganic Materials*, **40**, No. 6, 735-743 (2004).